Published in final edited form as:
Nat Med. 2011 June ; 17(6): 732–737. doi:10.1038/nm.2368.

Host mediated regulation of superinfection in malaria

Silvia Portugal[1,4], **Céline Carret**[1], **Mario Recker**[2], **Andrew E. Armitage**[3], **Lígia A. Gonçalves**[4], **Sabrina Epiphanio**[1,§], **David Sullivan**[5], **Cindy Roy**[6], **Chris I. Newbold**[3], **Hal Drakesmith**[3], and **Maria M. Mota**[1,4]

[1]Instituto de Medicina Molecular, Faculdade de Medicina da Universidade de Lisboa, 1649-028 Lisboa, Portugal

[2]Department of Zoology, University of Oxford, Oxford OX1 3PS, UK

[3]Weatherall Institute of Molecular Medicine, John Radcliffe Hospital, University of Oxford, Oxford OX3 9DS, UK

[4]Instituto Gulbenkian de Ciência, 2780-156 Oeiras, Portugal

[5]The Malaria Research Institute, W. Harry Feinstone Department of Molecular Microbiology and Immunology, The Johns Hopkins Bloomberg School of Public Health, Baltimore, MD 21205, USA

[6]Division of Geriatric Medicine and Gerontology, Johns Hopkins University School of Medicine, Baltimore, MD 21205, USA

Abstract

In regions of high malaria transmission, mosquitoes repeatedly transmit liver-tropic *Plasmodium* sporozoites into individuals who already have blood-stage parasitaemia[1]. This manifests itself in older semi-immune children by concurrent carriage of different parasite genotypes at low asymptomatic parasitaemias[2]. Superinfection presents an increased risk of hyperparasitaemia and death in less immune individuals, but counter-intuitively is not frequently observed in the young[3,4]. Here, we show in a rodent model, that ongoing blood-stage infections, above a minimum threshold, impair the growth of subsequently inoculated sporozoites such that they become growth arrested in liver hepatocytes and fail to develop into blood-stage parasites. Inhibition of the liver-stage can be mediated by the host iron regulatory hormone hepcidin[5], the synthesis of which is stimulated by blood-stage parasites in a density-dependent manner. We model this phenomenon and show how density-dependent protection against liver-stage malaria can shape the epidemiological patterns of age-related risk and complexity of malaria infections seen in young children. The interaction between these two *Plasmodium* stages and host iron metabolism has relevance for the global efforts to reduce malaria transmission and for nutritional programmes of iron supplementation in malaria-endemic regions.

Correspondence to M.M.M. (mmota@fm.ul.pt).
§current address: Departamento de Ciências Biológicas, Universidade Federal de São Paulo, Diadema, Brasil.

Note: Supplementary information, including full methods, is available on the Nature Medicine website.

AUTHOR CONTRIBUTIONS

S.P. performed the majority of the experimental work. C.C. performed the microarray analysis and M.R. and C.N. initiated and tested the mathematical model. L.A.G. produced murine primary hepatocytes. S.E., D.S. and C.R. provided intellectual input and C.R. provided *hamp1*-transgenic mice. M.M.M. has conceived and supervised the study. S.P., A.A., C.N., H.D. and M.M.M. designed the experimental procedures and wrote the manuscript. All authors read and approved the manuscript.

An infected mosquito bite transmits *Plasmodium* sporozoites that infect hepatocytes producing thousands of merozoites[6], that then infect red blood cells (RBCs) causing malaria[7]. In areas where malaria is endemic, individuals can be exposed to several hundred infected mosquito bites per year[1], conferring a risk of superinfection. In infants yet to acquire immunity and whose passively transferred maternal immunity has waned, individual infections result in potentially life-threatening episodes of disease[3]. Superinfections would be expected to elevate this risk (as different parasites may multiply independently causing lethal parasitaemias) but only if the sporozoites of a superinfection progressed as normal through the liver-stage in individuals that already have ongoing blood parasitaemia.

To address this question we utilised a rodent model of malaria where luciferase- and GFP-tagged parasites enable distinction between the original infection and the superinfection. We infected mice via mosquito bite with *P. berghei* parasites and after detecting parasites in the bloodstream (peripheral blood parasitemia 0.99±0.03%), we challenged the same mice by mosquito bite with luciferase-expressing *P. berghei*. Light emission correlates with *Plasmodium* liver load[8]. Liver-stage infection was dramatically inhibited in mice with ongoing blood-stage parasitaemia (Fig. 1a). The observed reduction in secondary *Plasmodium* liver infection depended on the ongoing blood-stage infection, as mice first infected with blood-stage parasites via blood transfusion, and later challenged via mosquito bite with luciferase-expressing *P. berghei* displayed a similar impairment in liver infection (Fig. 1b). Most strikingly, luciferase-labelled parasites never reached detectable levels in the blood (Fig. 1c). A potent and significant reduction in *P. berghei* liver load was confirmed and quantified in mice with an ongoing blood-stage infection and challenged with sporozoites constitutively expressing GFP (Fig. 1d); qRT-PCR of GFP *mRNA* was used as readout as GFP expression correlates with *Plasmodium* liver load (Supplementary Fig. 1). Again, GFP-expressing parasites were never detected in blood (Fig. 1e). This effect was neither species- nor strain-specific. Mice carrying blood-stage infections with *P. berghei* NK65, *P. berghei* ANKA, *P. chabaudi chabaudi* AS or *P. yoelii* 17X parasites and challenged with GFP-expressing *P. berghei* ANKA sporozoites showed a very strong reduction in liver-stage infection ($P<0.01$; Fig. 1d). Likewise, *P. berghei* NK65 blood-stage infection strongly inhibited liver-stage infection by GFP-expressing *P. yoelii* 17X sporozoites ($P<0.05$; Fig. 1f).

The decrease in liver parasite load was consistently observed from day 3 to day 14 of a blood-stage malaria infection started with 10^6 iRBCs, when parasitaemia remained above 1% (1.24±0.24 – 15.53±3.80%; $P<0.05$; Fig. 1g). Additionally, when blood-stage parasitaemia was initiated with increasing numbers of iRBCs (10^3–10^7 iRBCs) but all re-infected with *P. berghei* ANKA sporozoites on day 3, we observed significant impairment in liver-stage infection at parasitemias exceeding 0.15% (0.16±0.07 – 3.61±0.63%; $P<0.01$) (induced following inoculation of 10^5 iRBCs) ($P<0.05$; Fig. 1h). Conversely, if an ongoing blood-stage infection was treated with the antimalarial drug chloroquine or naturally cleared from circulation (as during *P. c. chabaudi* AS infections) then inhibition of liver-stage development was abrogated (Fig. 1i, j). These data suggest that the observed decrease in liver parasite only occurs above a certain critical threshold of blood parasite density.

We next investigated the nature of the inhibition of *Plasmodium* liver-stage by an ongoing blood-stage infection. Microscopic examination of thick liver sections from control and reinfected mice from 3 independent experiments clearly revealed that both the number and size of exo-erythrocytic forms (EEFs) decrease in the presence of blood-stage parasites when measured 40 to 48h after sporozoite inoculation (Fig. 2a–d and Supplementary Fig. 1). Together these reductions account for the overall impairment to liver-stage development and mimic the observed reduction in infection liver load quantified by qRT-PCR in the same livers (Fig. 2d). No EEFs were detectable 72h after sporozoite infection in mice with a blood-stage infection (Supplementary Fig. 1).

Altogether, these data indicate that inhibition of *Plasmodium* liver infection by an ongoing malaria blood-stage infection is independent of the *Plasmodium* species, transient, and results in small EEFs that fail to generate detectable blood-stage infections. The data are also consistent with a critical density threshold of blood-stage parasites inhibiting the development of the liver-stage, resembling a quorum sensing mechanism described for bacteria[9], by which the blood-stage is able to protect its niche from the threat of superinfection. We ruled out the possibility that a blood-stage secreted soluble factor was directly responsible for mediating inhibition since infection of both mouse primary hepatocytes and hepatoma cells by *P. berghei* sporozoites was unaffected by co-culture with iRBCs (Fig. 2e and Supplementary Fig. 2).

We next examined differences in host liver transcription between naïve mice (NI), sporozoite-infected mice (LS), mice carrying a blood-stage infection alone (BS) or after secondary sporozoite infection (Reinf) by genome-wide microarray analysis. Immune-related genes were upregulated in both BS and Reinf mice, and genes associated with a defense response, including several TLRs, chemokines, complement components or IFN regulatory factors were upregulated in the latter (Fig. 2f, Supplementary Fig. 3, and Supplementary Table 1), suggesting that a blood-stage initiated immune response might account for impaired liver-stage development. However, using either splenectomised mice, genetically deficient mice or depletion methods, we showed that the impairment of *Plasmodium* liver infection in the presence of blood-stage parasitaemia is independent of T or B cells; NK or γδ T cells; IFN-gamma, TNF-α, NOS, IL-10, IL-6, TLR/MyD88 signalling; the complement system or mastocytes (Fig. 2g–i and Supplementary Fig. 3). Lack of any of these independent components, or the administration of a general anti-inflammatory molecule (N-acetyl-cysteine) (Supplementary Fig. 3), did not even partially rescue the observed impairment. Moreover, luciferase-labelled parasites never reached detectable levels in the blood of immuno-depressed (SCID) re-infected mice. These data provide no support for a role of adaptive immunity or aspects of innate immunity in the phenotype observed. (Supplementary Fig. 3).

Plasmodium blood-stages increase apoptosis in hepatocytes[10] and microarray data shows a robust pro-apoptotic stimulus in the livers of mice with an ongoing blood-stage infection (Supplementary Table 1). However, although a significantly reduced level of apoptosis was observed in *P. berghei* NK65 blood-stage infected caspase-3 deficient mice (Supplementary Fig. 4), blood-stage infection in these mice still impaired a secondary *P. berghei* ANKA

liver infection ($P<0.05$; Fig. 2j). Thus, hepatocyte apoptosis does not explain the observed protection.

The reduction of both the number and size of EEF in the presence of a blood infection (Fig. 2a–c) suggested that some nutrient or growth factor might be limiting liver-stage development. Previous reports link iron availability and *Plasmodium* infection of both RBCs[11] and hepatocytes[12–14]. *hamp1*, the gene encoding the iron regulatory hormone hepcidin, is significantly over-expressed in the livers of mice with ongoing blood-stage infection (2.7-fold increase in Reinf by microarray analysis, $P<0.05$, Supplementary Table 1). We confirmed by qRT-PCR an average 5-fold increase in *hamp1* expression levels in mice with an ongoing blood-stage infection ($P<0.01$; Fig. 3a), consistent with previous findings of increased hepcidin in human blood-stage infection[15,16]. Importantly, hepcidin levels fully correlated with parasitemia and, above a certain threshold (3.3-fold hepcidin increase for 0.15% parasitemia), inversely correlated with *Plasmodium* liver infection ($P<0.01$; Fig. 3a). The increase in hepcidin *mRNA* depends on blood-stage parasitemia as it reverted to normal levels after chloroquine-treatment of infected mice (Fig. 3b) or after resolution of *P. c. chabaudi* AS infection (Supplementary Fig. 5), correlating with regained permissiveness to liver-stage re-infection (Fig. 1i, j). Hepcidin regulates iron homeostasis and distribution by targeting the iron exporter ferroportin for degradation, thereby preventing release of recycled RBC iron and dietary iron to serum from ferroportin-expressing macrophages and enterocytes respectively[5,17]. We showed that increased *hamp1* expression during blood-stage infection was associated with iron redistribution: increased levels of ferritin within liver macrophages (Fig. 3c), increased iron in the spleen and reduced iron in hepatocytes (Fig. 3d). IL-6 and bone-morphogenetic proteins (BMPs) are known hepcidin agonists[18,19]. Blood-stage infection increased expression of Id1 (Supplementary Fig. 5), a known BMP target gene[20] and *hamp1* upregulation in primary hepatocytes by sera of blood-stage infected mice was inhibited by dorsomorphin (Fig 3e), a BMP signaling antagonist[21]. Induction was also partially neutralized by anti-IL-6 antibodies (Fig 3e), suggesting that BMP and IL-6 pathways may synergize to induce hepcidin during a blood-stage infection.

Previous microarray analysis showed that ferroportin expression was significantly reduced in *Plasmodium*-infected hepatoma cells (47.0±0.2% reduction, $P<0.0001$), and the iron importer DMT1 was significantly increased (2.0±0.2 fold increase, $P<0.0001$)[22]. This suggests that iron acquisition and retention might be essential for complete *Plasmodium* development inside its host cells. Consistent with this, reducing iron availability in liver-derived cells using iron chelators bathophenanthrolinedisulfonate (BPS) and desferrioxamine (DFO) led to significant and dose-dependent inhibition of *Plasmodium* EEF development (Fig. 3f–h and Supplementary Fig. 5) whereas iron supplementation using Ferric Ammonium Citrate (FAC) dramatically increased development (Fig. 3g, h). These effects were reproduced in mice infected with *P. berghei* sporozoites (Fig. 3h).

Our data reveal that iron, necessary for complete *Plasmodium* sporozoite development, is significantly reduced in hepatocytes during a malaria blood-stage infection, presumably due to increased hepcidin expression. Thus, elevated hepcidin alone without ongoing blood-stage infection should inhibit *Plasmodium* liver infection. Accordingly, administration of

hepcidin peptide[17,23,24] prior to and after sporozoite infection significantly impaired liver infection (Fig. 3i). Additionally, two distinct hepcidin over-expression systems (*hamp1*-expressing adenovirus-infected mice and *hamp1*-transgenic mice[25], both causing a 2-fold increase in *hamp1* expression) showed that hepcidin significantly reduces liver-stage infection (Fig. 3i) to levels similar to those observed during blood-stage infections (Fig. 3a). Altogether, these data are consistent with an ongoing blood-stage infection stimulating hepcidin expression and consequently redistributing iron away from hepatocytes where it is required for successful *Plasmodium* EEF development (Fig. 3j).

We next asked what implications our observations in mice might have for human malaria, assuming the same phenomenon operates. Epidemiological studies from highly endemic areas consistently show that the incidence of infection first increases with age in young children before declining as a result of acquired immunity (e.g.[4,26]). In parallel, the complexity of infection, i.e. the average number of parasite clones per individual, also increases as hosts get older[4,26–28], so that older children frequently harbour asymptomatic infections consisting of multiple parasite genotypes[2], whereas superinfection is rarely encountered in infants, even though these individuals are less immune. To investigate if a threshold-density dependent inhibitory effect, such as we report here, could account for these counter-intuitive observations we devised a simple agent-based model. We simulated infection histories in a number of individuals, following them over time whilst recording the average annual infection rates and number of co-infecting clones (see Supplementary Information). According to epidemiological observations, the model assumes that the average parasite density per infection decreases with age[4, 27, 29]. The probability of an infectious bite initiating a new infection then depends on current blood-stage parasitemia together with the host's infection history. Under these minimal assumptions the model correctly predicts an initial increase in infection rates, which subsequently declines as individuals acquire immune protection through repeated exposure (Fig. 4a, c). We also observe an increase in the multiplicity of infection in older individuals as a consequence of higher infection risk and reduced inhibitory effect (Fig. 4b, d). We tested the model under various assumptions regarding the relationship between an ongoing blood-stage infection and the probability of superinfection and find that no other inhibitory effect can explain the observed data (Fig. 4a, b). The predictions of the model are also invariant to assumptions regarding age-dependent parasite clearance rates and maternal protection (Supplementary Fig. 6). This means that threshold-density dependent inhibition of new liver-stage infections alone can explain the changes in infection risk and complexity of infections in young individuals observed in the field. Crucially, however, our results show that this effect is strongly dependent on the transmission intensity and most prominently observed under moderate to high transmission settings (Fig. 4c and d). A previous attempt to explain these epidemiological observations[30] relied on the biting preference of mosquitoes towards older individuals. Our findings provide an alternative (or synergistic) mechanism underlying the differences in age-dependent risk of infection within the endemicity spectrum (Fig. 4f).

Host/pathogen/environment interactions can be extremely complex. For example, in order to maximize survival, some bacteria employ quorum-sensing[31], paracrine signalling[32] and even hormonal communication with their host (called inter-kingdom signalling[33]). Similarly

the intricacy of the *Plasmodium* life-cycle and its infection dynamics within host populations likely reflect behaviours that have been selected during co-evolution. Our results suggest a previously unsuspected aspect of this relationship, that blood-stage *Plasmodium* infections protect their erythrocyte niche from superinfection via the upregulation of a host hormone, hepcidin, which redistributes iron away from competitor liver-stage infections. This interaction acts independently of and in addition to acquired immunity and could resolve features of malaria epidemiology that have hitherto required speculative explanations (Fig 4f). It is possible that the mechanism we describe arose in order to maintain parasite density below life-threatening levels in non-immune individuals – benefitting both the host and the incumbent pathogen. The effect implies a balance of host iron levels, blood parasitaemia and the hepcidin response. One might therefore expect that altering iron availability could disturb these interactions. Indeed, a clinical trial of iron supplementation of under fives on Pemba island, Tanzania, where malaria is highly endemic, showed a statistically significant increase in malaria infections and risk of death in infants receiving iron[34]. Similarly, the profound and poorly explained anaemia that accompanies the disease may be partly due to the hepcidin response. Understanding how the life-stages of *Plasmodium* interact with the nutritional and immunological states of hosts of various ages may well benefit the current efforts to control malaria.

METHODS

Mice

Mice were bred in specific pathogen-free facilities at the Instituto de Gulbenkian de Ciência (Oeiras, Portugal). Rag2/gc deficient mice were kindly provided by James Di Santo (Institut Pasteur, Paris, France). Nos2- (B6.129P2-Nos2tm1Lau/J), Tcrd- (B6.129P2-Tcrdtm1Mom/J), and C5a- (B10.D2-Hc0.H2d.H2-T18c/oSnJ) deficient mice were purchased at The Jackson Laboratory along with respective wild type littermates. Mice were housed in the Instituto de Medicina Molecular (IMM) facilities and the IMM Animal Care Committee approved all protocols. Ifng deficient mice were kindly provided by Rui Appelberg (Instituto de Biologia Molecular e Celular-IBMC, Porto, Portugal) and experiments performed at IBMC after IBMC Animal Care Committee approved all protocols. All transgenic mice were genotyped by tail genomic DNA PCR to confirm their respective mutations.

Plasmodium blood infection

Primary blood-stage infection of mice was achieved by exposing mice for 30 minutes to 15 *Anopheles* mosquitoes infected with *P. berghei* ANKA, or by i.p. inoculation of the designated quantity of RBCs infected with *P. berghei* ANKA, *P. berghei* NK65, *P. yoelii* 17X NL or *P. chabaudi chabaudi* AS. Peripheral blood parasitaemia was determined by Giemsa staining followed by microscopic counting of iRBCs, real time *in vivo* imaging using the *in vivo* IVIS® Lumina Imaging System [8] (Fig. 1C) or flow cytometry of *gfp*-expressing parasites[35] (Fig. 1E). The results are expressed as percentage of infected RBCs.

Plasmodium liver infection

gfp-expressing or luciferase-expressing *P. berghei* ANKA and *gfp*-expressing *P. yoelii* sporozoites[8,35,36] were obtained by dissection of *Anopheles stephensi* infected mosquitoes bred at the IMM insectarium. Mice were infected i.v. with the designated quantity of sporozoites, or by 30 minutes exposure of mice to 15 infected *Anopheles* mosquitoes. Parasite liver load was quantified either by qRT-PCR or real time *in vivo* imaging using the *in vivo* IVIS® Lumina Imaging System[8].

Liver slice histopathology, morphometric analysis and immunofluorescence

Livers were harvested from control or re-infected mice 40 h after sporozoite infection, fixed in 4% paraformaldehyde for 15 minutes, washed and then sliced into 50 μm sections using a vibratome (VT1000S, Leica). Sections were permeabilized and blocked overnight in 0.3% Triton X-100 + 1% BSA and then incubated overnight at 4°C in the same solution containing anti-GFP IgG Alexa flour 488 congugate antibody, Alexa 594 phaloidin and 4′,6-diamidino-2-phenylindole (DAPI). After mounting 20 sections on slides, EEFs were counted on a Leica DM5000B Widefield Fluorescence Microscope, and the sizes of 20 randomly chosen EEFs per mouse were measured using a Zeiss LSM 510 META Point Scanning Confocal Microscope. Images of immunofluorescence-stained sections were analysed using the ImageJ 1.42b software. Areas and numbers of EEF were normalized to the total area observed.

Liver hepcidin (*hamp1*) quantification

Liver *hamp1* mRNA expression was determined by TaqMan qRT-PCR using inventoried TaqMan gene expression assays (*hamp1* - Mm00519025_m1; *gapdh* (Glyceraldehyde-3-phosphate dehydrogenase) - Mm99999915_g1) and TaqMan Gene Expression Master Mix (both Applied Biosystems) according to the manufacturer's instructions. qRT-PCR was performed using an ABI Prism 7500FAST system. Changes in *hepcidin* mRNA expression between control and re-infected mouse livers were calculated using the 2^{-DDCt} method with *gapdh* as the endogenous control gene.

Ferritin staining

Livers sections, prepared and fixed as described above, were incubated overnight at 4°C with rabbit anti-mouse heavy and light ferritin chain antibody (a kind gift by Paolo Arosio, Faculty of Medicine, Brescia, Italy) and Alexa 660 phaloidin (Invitrogen). After washing, sections were incubated for 6h with secondary Alexa fluor 595 donkey anti-rat IgG (Invitrogen) and DAPI (Sigma).

Iron treatments

Huh7 cells were incubated with Ferric Ammonium Citrate (FAC, Sigma) bathophenanthrolinedisulfonate (BPS, Acros) or Desferrioxamine (DFO, Sigma) solutions at designated concentrations (or diluents as control) 24h prior to sporozoite infection and infection measured by FACS 36h after infection. For i*n vivo* experiments, mice were inoculated i.p. with 250 mg/Kg of DFO or FAC 24h prior to sporozoite infection and parasite liver load measured 40h after infection.

Hepcidin induction

Hepcidin induction was achieved by (i) direct administration of *hamp1* peptide (Peptide, Japan) 20h prior to sporozoite infection and 20h after sporozoite infection, (ii) *hamp1*-expressing adenoviral administration (pAd.CMV.Hamp.ires.GFP.Wpre (HAMP.adV) kindly provided by Stefano Rivella, Weill Cornell Medical College, USA) 48h prior to sporozoite infection or (iii) expression of human *hamp1* transgene in mice[25]. Livers were collected 40 h after infection and parasite liver load determined by expression of PbA 18S *rRNA*.

Model description

A stochastic, individual-based model was used to follow a cohort of *N* individuals for up to 20 years in low, medium and high transmission settings (with according annual EIR of 2, 20 and 200, respectively). At each time point t_i the probability of an individual becoming infected, *P*, is given as the product of the probability of being bitten by an infected mosquito, p_{bite} (=1-1/EIR), times the probability of this bite leading to successful blood-stage infection which itself is dependent on the immune history of the host, p_{imm}, and the parasite density of a possible ongoing infection, p_{dens}. That is, $P(\text{infection}) = P(p_{bite} \cap p_{imm} \cap p_{dens})$. More detailed model description in Supplementary Information online.

Statistical analysis

All experiments were performed with at least 5 mice per group. Displayed results are either one representative of or the cumulative result of at least three independent experiments. Statistical analysis was performed using unpaired Student t or variance (ANOVA) parametric tests; normal distributions were confirmed using the Kolmogorov-Smirnov test. Significance is indicated by * and its value is identified in every graph.

Supplementary Material

Refer to Web version on PubMed Central for supplementary material.

Acknowledgments

We would like to thank Laurent Renia (Agency for Science, Technology and Research, Singapore) for helpful comments and reagents, as well as Rui Appelberg (Instituto de Biologia Molecular e Celular, Porto, Portugal), James Di Santo (Institut Pasteur, Paris, France) and Juan Rivera (National Institutes of Arthritis and Musculoskeletal and Skin Diseases, Bethesda, USA) for IFN-γ, RAG2/γ_C and Kit W-sh transgenic mice, Stefano Rivella (Weill Cornell Medical College, New York, USA) for GFP and HAMP.GFP-expressing adenovirus, and Paolo Arosio, (Faculty of Medicine University of Brescia, Italy) for anti-mouse heavy and light ferritin chain antibody.

This work was supported by Fundação para a Ciência e Tecnologia (FCT, Portugal), European Science Foundation (EURYI to MMM), Howard Hughes Medical Institute and the Medical Research Council UK. H.D. is a Beit Memorial Fellow for Medical Research and an MRC New Investigator. S.P. and C.C. were supported by FCT fellowships (SFRH/BD/31523/2006 and SFRH/BPD/40965/2007 respectively). M.R. is supported by a Royal Society University Research Fellowship.

References and Notes

1. Robert V, et al. Malaria transmission in urban sub-Saharan Africa. Am J Trop Med Hyg. 2003; 68:169–176. [PubMed: 12641407]

2. al-Yaman F, et al. Reduced risk of clinical malaria in children infected with multiple clones of Plasmodium falciparum in a highly endemic area: a prospective community study. Trans R Soc Trop Med Hyg. 1997; 91:602–605. [PubMed: 9463681]
3. Smith TA, Leuenberger R, Lengeler C. Child mortality and malaria transmission intensity in Africa. Trends Parasitol. 2001; 17:145–149. [PubMed: 11286800]
4. Molineaux, L.; Gramiccia, G. The Garki project: research on the epidemiology and control of malaria in the Sudan Savanna of West Africa. World Health Organization; Geneva: 1980.
5. Ganz T. Hepcidin--a peptide hormone at the interface of innate immunity and iron metabolism. Curr Top Microbiol Immunol. 2006; 306:183–198. [PubMed: 16909922]
6. Prudencio M, Rodriguez A, Mota MM. The silent path to thousands of merozoites: the Plasmodium liver stage. Nat Rev Microbiol. 2006; 4:849–856. [PubMed: 17041632]
7. Haldar K, Murphy SC, Milner DA, Taylor TE. Malaria: mechanisms of erythrocytic infection and pathological correlates of severe disease. Annual review of pathology. 2007; 2:217–249.
8. Ploemen IH, et al. Visualisation and quantitative analysis of the rodent malaria liver stage by real time imaging. PLoS One. 2009; 4:e7881. [PubMed: 19924309]
9. Henke JM, Bassler BL. Bacterial social engagements. Trends Cell Biol. 2004; 14:648–656. [PubMed: 15519854]
10. Guha M, Kumar S, Choubey V, Maity P, Bandyopadhyay U. Apoptosis in liver during malaria: role of oxidative stress and implication of mitochondrial pathway. Faseb J. 2006; 20:1224–1226. [PubMed: 16603602]
11. Heppner DG, Hallaway PE, Kontoghiorghes GJ, Eaton JW. Antimalarial properties of orally active iron chelators. Blood. 1988; 72:358–361. [PubMed: 3291984]
12. Goma J, Renia L, Miltgen F, Mazier D. Effects of iron deficiency on the hepatic development of Plasmodium yoelii. Parasite. 1995; 2:351–356. [PubMed: 8745736]
13. Goma J, Renia L, Miltgen F, Mazier D. Iron overload increases hepatic development of Plasmodium yoelii in mice. Parasitology. 1996; 112 (Pt 2):165–168. [PubMed: 8851855]
14. Stahel E, et al. Iron chelators: in vitro inhibitory effect on the liver stage of rodent and human malaria. Am J Trop Med Hyg. 1988; 39:236–240. [PubMed: 3052118]
15. Armitage AE, Pinches R, Eddowes LA, Newbold CI, Drakesmith H. Plasmodium falciparum infected erythrocytes induce hepcidin (HAMP) mRNA synthesis by peripheral blood mononuclear cells. Br J Haematol. 2009
16. de Mast Q, et al. Assessment of urinary concentrations of hepcidin provides novel insight into disturbances in iron homeostasis during malarial infection. J Infect Dis. 2009; 199:253–262. [PubMed: 19032104]
17. Nemeth E, et al. Hepcidin regulates cellular iron efflux by binding to ferroportin and inducing its internalization. Science. 2004; 306:2090–2093. [PubMed: 15514116]
18. Babitt JL, et al. Modulation of bone morphogenetic protein signaling in vivo regulates systemic iron balance. J Clin Invest. 2007; 117:1933–1939. [PubMed: 17607365]
19. Nemeth E, et al. Hepcidin, a putative mediator of anemia of inflammation, is a type II acute-phase protein. Blood. 2003; 101:2461–2463. [PubMed: 12433676]
20. Katagiri T, et al. Identification of a BMP-responsive element in Id1, the gene for inhibition of myogenesis. Genes Cells. 2002; 7:949–960. [PubMed: 12296825]
21. Yu PB, et al. Dorsomorphin inhibits BMP signals required for embryogenesis and iron metabolism. Nat Chem Biol. 2008; 4:33–41. [PubMed: 18026094]
22. Albuquerque SS, et al. Host cell transcriptional profiling during malaria liver stage infection reveals a coordinated and sequential set of biological events. BMC Genomics. 2009; 10:270. [PubMed: 19534804]
23. Drakesmith H, et al. Resistance to hepcidin is conferred by hemochromatosis-associated mutations of ferroportin. Blood. 2005; 106:1092–1097. [PubMed: 15831700]
24. Rivera S, et al. Synthetic hepcidin causes rapid dose-dependent hypoferremia and is concentrated in ferroportin-containing organs. Blood. 2005; 106:2196–2199. [PubMed: 15933050]
25. Roy CN, et al. Hepcidin antimicrobial peptide transgenic mice exhibit features of the anemia of inflammation. Blood. 2007; 109:4038–4044. [PubMed: 17218383]

26. Sama W, Owusu-Agyei S, Felger I, Dietz K, Smith T. Age and seasonal variation in the transition rates and detectability of Plasmodium falciparum malaria. Parasitology. 2006; 132:13–21. [PubMed: 16393349]
27. Mayor A, et al. Plasmodium falciparum multiple infections in Mozambique, its relation to other malariological indices and to prospective risk of malaria morbidity. Trop Med Int Health. 2003; 8:3–11. [PubMed: 12535242]
28. Owusu-Agyei S, Smith T, Beck HP, Amenga-Etego L, Felger I. Molecular epidemiology of Plasmodium falciparum infections among asymptomatic inhabitants of a holoendemic malarious area in northern Ghana. Trop Med Int Health. 2002; 7:421–428. [PubMed: 12000651]
29. Mmbando BP, et al. Epidemiology of malaria in an area prepared for clinical trials in Korogwe, north-eastern Tanzania. Malar J. 2009; 8:165. [PubMed: 19615093]
30. Smith T, et al. Relationship between the entomologic inoculation rate and the force of infection for Plasmodium falciparum malaria. Am J Trop Med Hyg. 2006; 75:11–18. [PubMed: 16931811]
31. Fuqua C, Winans SC, Greenberg EP. Census and consensus in bacterial ecosystems: the LuxR-LuxI family of quorum-sensing transcriptional regulators. Annu Rev Microbiol. 1996; 50:727–751. [PubMed: 8905097]
32. Lopez D, Vlamakis H, Losick R, Kolter R. Paracrine signaling in a bacterium. Genes Dev. 2009; 23:1631–1638. [PubMed: 19605685]
33. Hughes DT, Sperandio V. Inter-kingdom signalling: communication between bacteria and their hosts. Nat Rev Microbiol. 2008; 6:111–120. [PubMed: 18197168]
34. Sazawal S, et al. Effects of routine prophylactic supplementation with iron and folic acid on admission to hospital and mortality in preschool children in a high malaria transmission setting: community-based, randomised, placebo-controlled trial. Lancet. 2006; 367:133–143. [PubMed: 16413877]
35. Franke-Fayard B, et al. A Plasmodium berghei reference line that constitutively expresses GFP at a high level throughout the complete life cycle. Mol Biochem Parasitol. 2004; 137:23–33. [PubMed: 15279948]
36. Tarun AS, et al. Quantitative isolation and in vivo imaging of malaria parasite liver stages. Int J Parasitol. 2006; 36:1283–1293. [PubMed: 16890231]

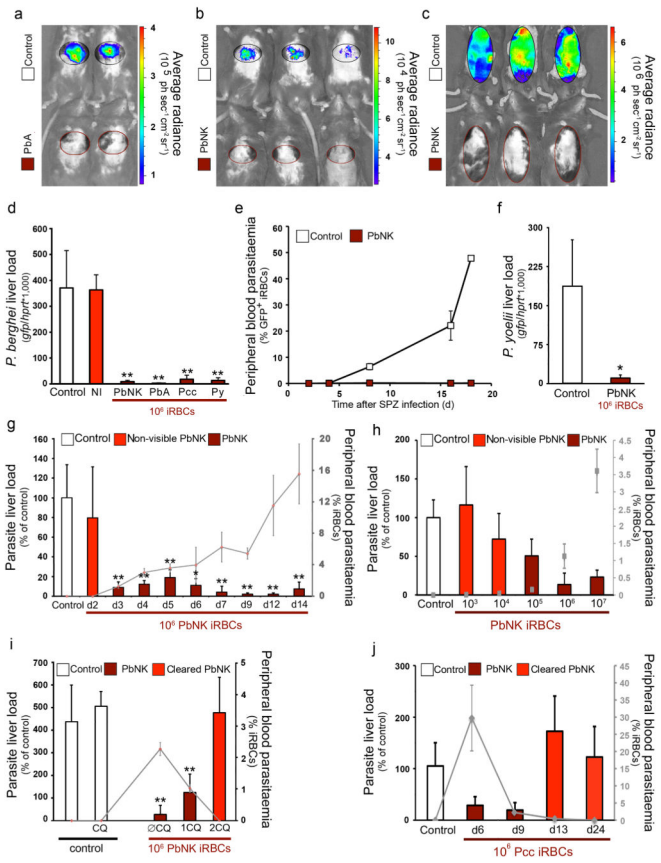

Figure 1. Malaria blood-stage infection protects against secondary *Plasmodium* liver infection

Plasmodium load measurement after sporozoite infection of naive mice (Control) or mice previously infected with *P. berghei* ANKA (PbA), *P. berghei* NK65 (PbNK), *P. chabaudi* AS (Pcc) or *P. yoelii* 17X (Py). Grey lines and squares represent peripheral blood parasitaemia at the time of re-infection. (**a**) 40h after luciferase-expressing PbA infective mosquito bites of mice infected 6 days before with PbA infective mosquito bites. (**b**) 40h after luciferase-expressing PbA infective mosquito bites of mice infected 5 days before with 10^6 PbNK iRBCs. (**c**) as in (b) but 3 days later. (**d**) 40h after 5×10^4 PbA-GFP sporozoite infection of mice injected 5 days before with non-infected blood (NI), or 10^6 PbA, PbNK, Pcc or Py iRBCs. (**e**) Peripheral blood parasitaemia after 5×10^4 PbA-GFP sporozoite infection of mice infected 5 days before with 10^6 PNK65 iRBCs. (**f**) 40h after Py-GFP sporozoite infection of mice infected 5 days before with PNK65 iRBCs. (**g**) 40h after PbA-GFP sporozoite infection of mice infected 2–14 days before with PbNK iRBCs. (**h**) 40h after Pb A-GFP sporozoite infection of mice infected 3 days before with $10^{3–7}$ PbNK iRBCs. (**i**) 40h after PbA-GFP sporozoite infection of mice infected 5 days before with PbNK iRBCs; with or without chloroquine treatment for 1 or 2 days before sporozoite injection (1CQ, 2CQ and ØCQ respectively). (**j**) 40h after PbA-GFP sporozoite infection of mice infected 6, 9, 13 or 24 days before with Pcc iRBCs. (**P* <0.05; ***P* <0.01, Ttest). Results expressed as mean ±s.d. of 3 independent infections (n≥5 mice per group).

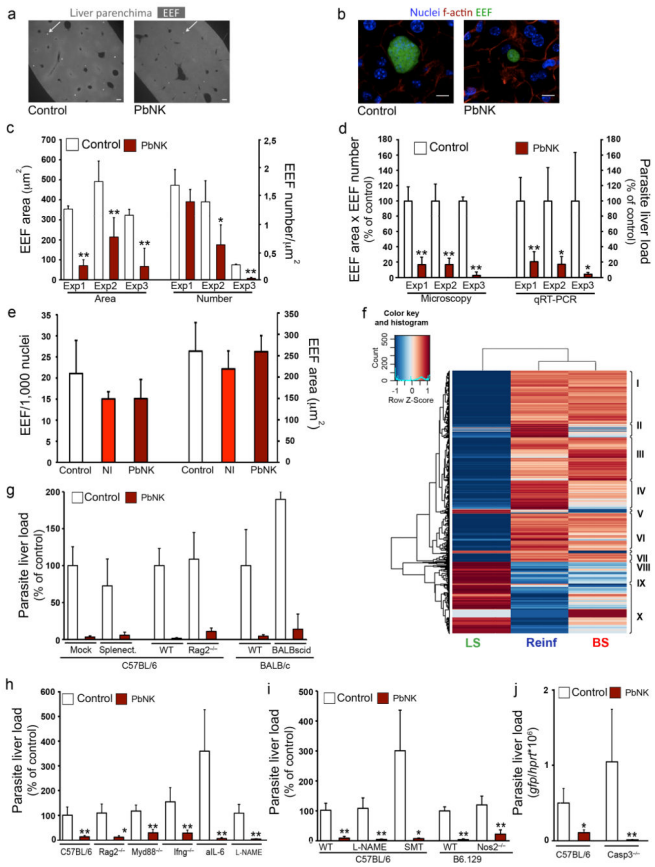

Figure 2. Effect of blood-stage infection on superinfecting sporozoite EEF number/development and sporozoite-infection of hepatocytes

Plasmodium load measurement after sporozoite infection of naïve mice (Control) or mice previously infected with *P. berghei* NK65 (PbNK). (**a**) Liver sections, 40h after 2×10^5 PbA-GFP sporozoite infection of mice infected 5 days before with 10^6 PbNK iRBCs; arrows exemplify EEFs (bar = 100µm). (**b**) Representative EEF in liver sections from (a) (bar = 10µm.). (**c**) EEF size (Area) and density (Number) of three independent experiments as described in (a). (**d**) Comparison of microscopy and qRT-PCR quantification of three independent experiments as described in (a). (**e**) 40h after 2×10^4 PbA-GFP sporozoite infection of mouse primary hepatocytes co-cultured with non-infected RBCs (NI) or 6×10^5 PbNK iRBCs. (**f**) Heatmap showing Differentially Expressed transcripts of infected *vs* non-infected mice, Gene Ontology enriched clusters pointed in roman, ($P<0.05$, Fisher Exact Test One Tail). (BS: blood-stage, LS: liver-stage, Reinf: re-infection). (**g**–**j**) 40h after 5×10^4 PbA-GFP sporozoite infection of mice infected 5 days before with 10^6 PbNK iRBCs. Experiments were performed in groups of splenectomised mice (Splenect.), genetically deficient mice ($Rag2^{-/-}$, $Myd88^{-/-}$, $Ifng^{-/-}$, $Nos2^{-/-}$ or $Casp3^{-/-}$) or after cell-depletion with anti-IL6 monoclonal antibody (aIL-6), or drug treatments with Nω-Nitro-L-arginine methyl ester hydrochloride (L-NAME) or S-methylthiourea (SMT). (*P <0.05; **P <0.01, Ttest). Results expressed as mean±s.d. of 3 independent infections (n≥5 mice per group).

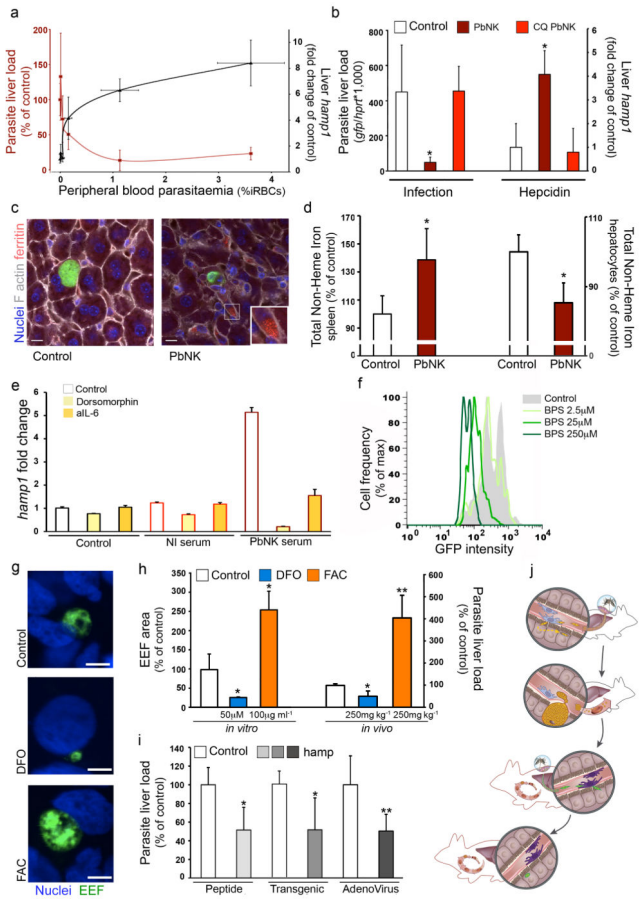

Figure 3. Hepcidin increase induction during blood stageblood-stage infection leads to iron redistribution and restricts *Plasmodium* liver infection

Plasmodium load and relative *hamp1* expression measurements after sporozoite infection of naïve mice (Control) or mice previously infected with *P. berghei* NK65 (PbNK). (**a**) Liver load (red), relative *hamp1* expression (black) and peripheral blood parasitaemia (x-axis), 40h after PbA-GFP sporozoite injection of mice infected 3 days before with $10^{3–7}$ PbNK iRBCs. (**b**) 40h after PbA-GFP sporozoite infection of mice infected 5 days before with 10^{6} PbNK iRBCs, with or without 2 days chloroquine treatment (CQ). (**c**) EEF and ferritin distribution in livers as in (b) (bar = 10μm.). (**d**) Total non-heme iron quantification of spleen (left axis) and liver hepatocytes (right axis) as in (b). (**e**) *Hamp1* expression of mouse primary hepatocytes 24h post-treatment with serum from non-infected mice (NI serum) or PbNK infected mice (PbNK serum), in the presence of dorsomorphin or IL-6 depleting antibody (aIL-6). (**f**) 36h after PbA-GFP sporozoite infection of Huh7 hepatoma cells in the presence of bathophenanthrolinedisulfonate (BPS). Plot shows one representative dataset of triplicate samples. (**g–h**) Effect of Desferrioxamine (DFO) and Ferric Ammonium Citrate (FAC) on *Plasmodium* infection in Huh7 hepatoma cells and liver infection. Representative images (g), EEF area quantification (h, left axis) 36h after PbA-GFP sporozoite infection or *Plasmodium* liver load (h, right axis) 40h after PbA-GFP sporozoite injection of pre-treated mice. (bar = 10μm.) Results are expressed as the mean ± s.d. of 3 independent infections. (**i**) 40h post PbA sporozoite injection of mice treated with human hepcidin peptide (Peptide); of

mice expressing a human *hamp* transgene (Transgenic); and of mice infected with *hamp* expressing adenovirus. (**j**) Schematic representation of hepcidin-mediated iron redistribution and regulation of superinfection in malaria. (**P* <0.05; ***P* <0.01, Ttest). Results expressed as mean±s.d. of 3 independent infections (n≥5 mice per group).

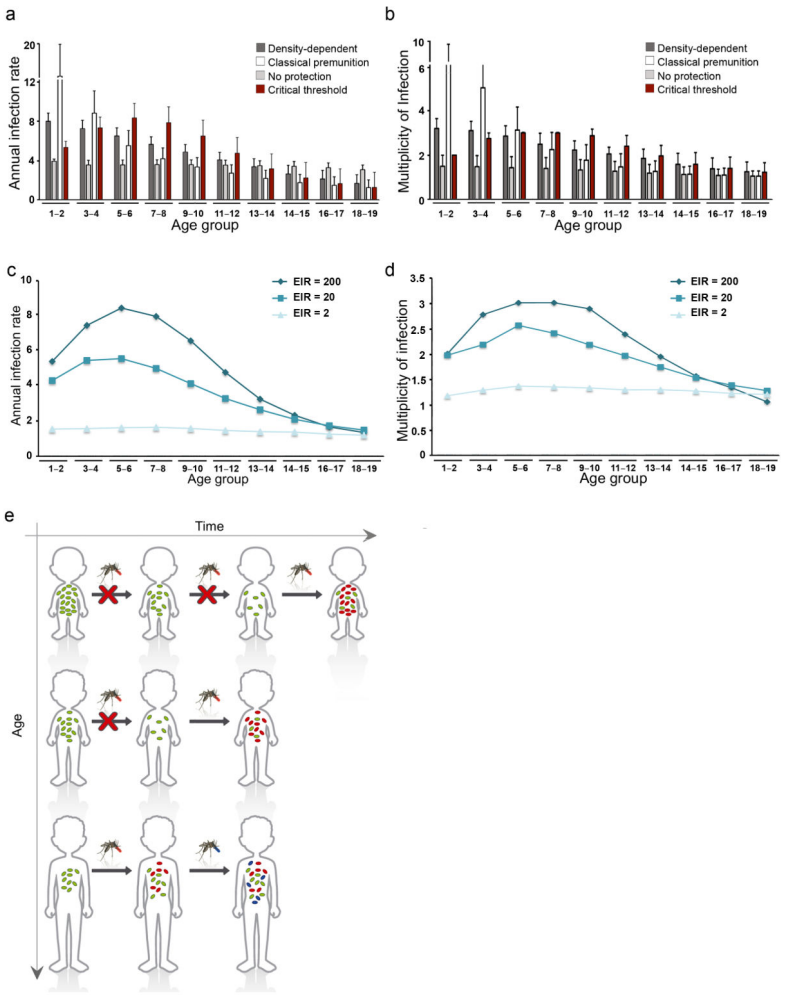

Figure 4. Model predictions for age-related incidence and multiplicity of infections

(**a** and **b**) Four different assumptions were tested regarding a possible inhibitory effect of a blood-stage infection: (i) density-dependent, where the probability of infection directly correlates with parasite density; (ii) classical premunition, where a new infection can only be established after an ongoing infection is essentially cleared; (iii) no protection, where the probability of infection is independent of an ongoing infection; and (iv) critical threshold dependent, where a new infection can only be established once the blood-stage parasite density falls below a certain level. (**c** and **d**) The results reveal a strong dependency on transmission intensities and predict that the observed age-dependency in the rates of infection and multiplicity are lost under low levels of transmission. (**e**) Schematic representation of parasite-dependent protective effect over age and time. Malaria infections in young children are often characterised by high levels of blood-stage parasitaemia that protect them against superinfections. Infected individuals thus become susceptible to further infections only once parasite densities fall below a critical threshold, reducing both the overall infection rate and probability of multi-clonal infections in young children. As they grow older, however, their typical blood parasitaemia levels drop and they more rapidly lose the protective effect against superinfection. As a result, successive infections become more

frequent and more likely to occur before an ongoing blood-stage infection is cleared, which then causes the observed increase in multiplicity of infection.